Incorporating Physics-based Models into Data Driven Approaches for Air Leak Detection in City Buses

Yuantao Fan[0000−0002−3034−6630], Hamid Sarmadi[0000−0002−7209−9623], and Sławomir Nowaczyk[0000−0002−7796−5201]

Center for Applied Intelligent System Research, Halmstad University
{firstname.lastname}@hh.se

Abstract. In this work-in-progress paper two types of physics-based models, for accessing elastic and non-elastic air leakage processes, were evaluated and compared with conventional statistical methods to detect air leaks in city buses, via a data-driven approach. We have access to data streamed from a pressure sensor located in the air tanks of a few city buses, during their daily operations. The air tank in these buses supplies compressed air to drive various components, e.g. air brake, suspension, doors, gearbox, etc. We fitted three physics-based models only to the leakage segments extracted from the air pressure signal and used fitted model parameters as expert features for detecting air leaks. Furthermore, statistical moments of these fitted parameters, over predetermined time intervals, were compared to conventional statistical features on raw pressure values, under a classification setting in discriminating samples before and after the repair of air leak problems. The result of this exploratory study, on six air leak cases, shows that the fitted parameters of the physics-based models are useful for discriminating samples with air leak faults from the fault-free samples, which were observed right after the repair was performed to deal with the air leak problem. The comparison based on ANOVA F-score shows that the proposed features based on fitted parameters of physics-based models outrank the conventional features. It is observed that features of a non-elastic leakage model perform the best.

Keywords: Fault detection, Air Leaks, Elastic air leakage model, Non-elastic air leakage model, Physics-informed machine learning, Explainable Predictive Maintenance

1 Introduction

Predictive maintenance enables a cost-effective approach for maintaining industrial equipment and helps ensure high operational performance as well as adherence to safety requirements. Different aspects of monitoring and analysis, such as fault detection, identification or estimation of remaining useful life, can be done using data-driven techniques that leverage historical data of the equipment.

Approaches based on Machine Learning (ML) algorithms have shown promising performance and were adopted by many industrial applications. Lately, deep neural networks have became very popular among researchers, however, industrial adoption is somewhat slower; one disadvantage of this approach is that it needs a great amount of training data (i.e., it is not very data-efficient), with a representative population including both normal operation data as well as fault and failure cases. Furthermore, inferences and predictions made with deep learning methods often lack interpretability and explanations of the decisions made.

Recently, a new trend has been developing to make ML methods more effective and data-efficient: to take advantage of models inspired by physics knowledge [10, 11, 9]. Physics-based models aim to calculate physical parameters from sensor data or outputs of ML models. These calculated parameters are employed to reduce workload on the ML model while increasing its explainability. This trend builds on decades-long desire to infuse data-driven reasoning with existing (often partial) domain knowledge, as opposed to requiring computers to learn completely from scratch. As a consequence of higher explainability, it is also easier to use physics-based ML models for enforcing, for example, policies or regulatory laws [7]. The calculated physics-based parameters can reduce the complexity of the problem for the ML-based method and hence improve the efficiency of the whole prognosis system. Another advantage is capability to do prognosis over an extended period of time, which might not be possible with purely ML-based methods when training samples come from a limited length of observation [8].

In the literature, several different approaches to combining ML and physics-based models have been proposed. One example is reducing the dimensions of the output space through orthogonal decomposition [9]. Another common approach is generating extra inputs for the learning method (i.e, virtual sensors) based on the values of other inputs [5, 3, 2]. A common theme among many works is the usage of recurrent neural networks (RNNs), including LSTM, which makes it possible to directly use the differential equations prevalent in physics-based modeling [10].

The case study presented in this paper focuses on detecting leak-related faults in a vehicle air system. The vehicle air supply, and the corresponding distribution system, were designed to provide compressed air to drive various components, e.g., air brakes, suspension, doors, gearbox, etc. The air pressure is regulated within a predefined range which is of crucial importance for the driver since without compressed air the vehicle will not operate. Air leaks in the system, depending on the severity, may render a lower operation efficiency, and, in the worst case, compromise the braking system, and thus jeopardize overall safety. The specific case presented in this study is based on a commercial fleet of buses, of the same model, driving in city and intercity traffic. Previous work on predicting air compressor failures in the same fleet by incorporating expert knowledge, using the charging rate of the air pressure as an expert feature, for predicting air compressor failures, is available in [4]. The air leak events (the time

of the occurrences, the types of the leakage, and any additional relevant details) were inferred from the vehicle service record. The six air leak cases included in this study have occurred in four buses, during their daily operation. Repairs were performed in a workshop to deal with the air leak problems. It is crucial to point out that the information is quite limited, and details such root cause or fault mode are approximate at best – there is no guarantee that all six cases exhibit similar symptoms. We have acquired sensor data of three months for each of these cases, around the repair date, for analysis. Naturally, we label the samples prior to the repair as faulty, and samples following the repair as healthy, or fault-free.

In this study, we have investigated the use of two types of physics-based model, namely elastic and non-elastic air leakage models. They are used to generate expert features suitable for detecting air leaks. The general idea is to fit these physical models to the pressure data, during the leakage periods, and estimate the model parameters that correspond to current physical properties. One particular challenge is that we do not have access to the exact system schematic design, nor did a dedicated simulator for the underlying physical process of the air system is available. In earlier work those were typically considered prerequisites for using physics-based techniques. The nature of the six air leaks were also not available, such as the exact location or type of the air leak. Therefore, it is not known a priori which physics-based model (e.g., elastic or non-elastic leakage) they correspond to. Finally, the number of the air leak cases available is not sufficient to train an effective machine learning model for fault detection or prognosis.

The contribution of this exploratory study is to evaluate and compare the usefulness of two relevant physics-based leakage models in detecting real air leak cases for city buses. The fitted parameters of the physics-based models are used as expert features, and the performance of these features is evaluated for discriminating faulty samples from fault-free ones. The results show that, in three out of the six cases, the fitted parameters are useful for the fault detection task. Furthermore, it is shown that the statistical features computed using the fitted parameters of the physics-based models outperform the conventional statistical features computed directly from the raw sensor data.

2 Background

The air system on-board buses in this fleet consist of the supply system, the control system, the distribution network, and the end-use components that consume the air for different purposes. A conceptual diagram of the air system in the city buses investigated in this study was illustrated in Figure 1. Compressed air flow was generated from the air compressor, and afterward regulated, dry filtered, and supplied to the air tank, which serves as a reservoir to store and facilitates the air supply when needed. The air pressure was maintained within a certain range, normally from 10 to 12 bars, to ensure the air demand of the end-use components was always met. Whenever the air pressure dropped below the

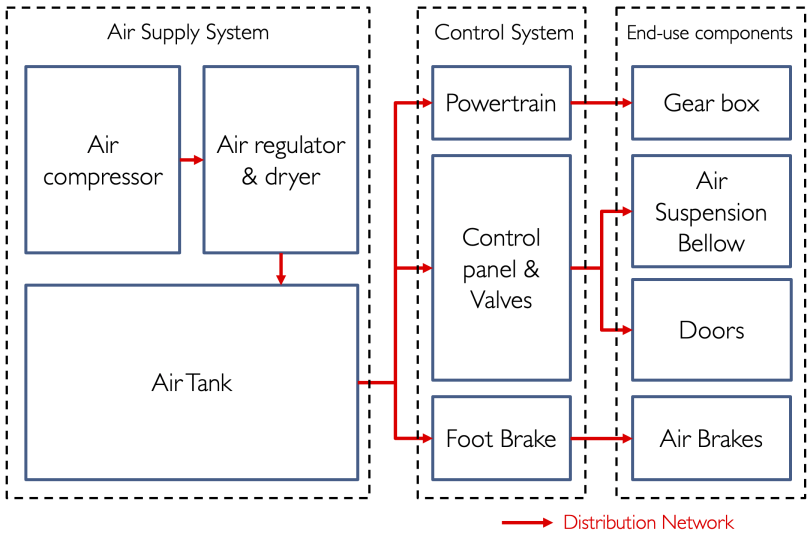

Fig. 1: A conceptual diagram of the air system in this study

bottom threshold, the compressor started charging the air into the system until the upper bound of the pressure level is reached. Through the control system (e.g., foot brake, valves, buttons, etc.), the operator determines the usage of the air, to activate different end-use components, e.g., air brake, doors, suspension bellows, gearbox, etc.

The only observation directly available for monitoring the air system behavior is the *Wet Tank Air Pressure* (WTAP), collected via a pressure sensor placed in the air tank. This data stream was accessed through the vehicle CAN network. The brake pedal position and selected gear were available as the control signals. The availability of the control signals varies over different time periods and buses in the fleet. Unfortunately, the signal indicating the door operation was not available for these buses. On the other hand, it can be derived, at least with some level of approximation, from the GPS signal and the vehicle speed. Figure 2 shows the pressure signal in the air tank, and the associated activation of the end-use components, derived from the control signals.

Air leaks may occur at various locations within the air system; the leakage mechanism and the cause of it may vary. In this work, we focus on the six air leak cases: i) bus A had leaks in the pipe and in the air bellow; ii) bus B had its air regulator replaced due to malfunctioning once it was unable to meet the operation requirements; iii) after 14 weeks, bus B had reports of leaks in the air bellows; iv) the fleet operator reported that there was a compressed air leak in Bus C, and the bus would not start; v) After ten months, bus C was reported to exhibit leaks in the air bellows; vi) oil and water were found to have leaked into the air tank through other components in bus D. In this study, we focus on the two-month period before and after the repair event, and on the air

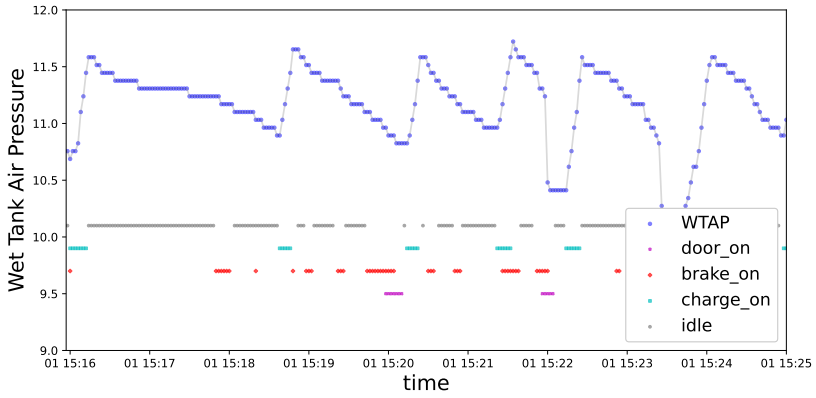

Fig. 2: Wet Tank Air Pressure (WTAP) and the corresponding activities of different vehicle components (represented as horizontal bars of various colors).

leakage faults. Samples prior to the repair event were labeled as faulty, and the subsequent samples after the repair event were labeled as fault-free, i.e., healthy.

3 Method

In this study, since the exact model of the faults is unknown, we analyze three physics-based models: one non-elastic leakage model, and two variants of elastic leakage models.

The first step in the proposed approach is to identify the portions of the data where the system behaves in as simple as possible way. Particularly in the case of vehicle air system, different components use the air in very different fashion, and the specific often depend, in quite complex manner, on external circumstances. Those internal control processes are too complex to model here, and they often use inputs that are not available in the data collected from CAN network. Therefore, we have decided to identify segments where none of the end-usage components are active. In a perfect world, this means WTAP signal should remain constant during those periods – any change in value can be attributed to a leak. Moreover, the parameters of any such potential leak are going to be the most clearly visible, and easiest to estimate. Therefore, the model parameters were estimated during such "leakage segments" extracted from the air pressure signal, and statistical features of the fitted parameters were adopted as expert features for air leak detection.

3.1 Physics-based Air Leakage Models

We take advantage of a formula inspired by the physics of leakage. The formula of the leak rate [6] of a vessel is defined by:

$$R = -V\frac{\mathrm{d}P_v}{\mathrm{d}t}, \tag{1}$$

where R is the leak rate, V is the volume of the vessel, P_v is the pressure inside the vessel, and t represents time. Also, assuming the leak is big enough to have a non-molecular flow the leak rate can be approximated [1] as:

$$R = L(P_v - P_o), \tag{2}$$

where L is called "leak size" and is proportional to the area of the leak, and P_o is the pressure outside of the leakage. Equating the two formulas leads to:

$$-V\frac{\mathrm{d}P_v}{\mathrm{d}t} = L(P_v - P_o). \tag{3}$$

Solving the differential equation and assuming L, P_o and V are constant, we obtain:

$$P_v = k\left[\exp\left(-\frac{L}{V}t\right)\right] + \frac{LP_o}{V}. \tag{4}$$

Since there might be also elastic leaks (e.g., in the seals of the vessel), we simulate them by assuming that P_o can be higher than its actual value. Therefore, we can re-parameterize the formula to account for a general leak:

$$P_v = k\left[\exp\left(-at\right)\right] + b \tag{5}$$

This way one can fit the data to our physics-inspired model simply by estimating the three parameters: a, b, and k.

An alternative way of modeling elastic leaks is to make the leak size pressure-dependent. For this purpose, we define:

$$L = \alpha(P_v - P_o)^2 \tag{6}$$

This leads to the following solution to Equation 3:

$$P_v = \frac{1}{\frac{\alpha}{V}t + C} + P_o, \tag{7}$$

where C is a constant. After re-parametrization we get:

$$P_v = \frac{1}{mt + n} + P_o. \tag{8}$$

To summarize, in this study we investigate the use of a non-elastic leakage model (equation 4) and two elastic leakage models (equations 5 and 8) for detecting air leak events.

3.2 Fitting Model Parameters

Conceptually, the *Wet Tank Air Pressure* signal is affected by all components within the air system: i) during the charging period the compressor charges the air into the air tank and raises the pressure; ii) during the air releasing period the end-use components use the air; iii) and as one would expect, during the period when none of the components are activated, the pressure changes only due to air leakage. The air pressure segments without any components in use were extracted for analysis.

The pressure values are denoted as $x^i_{v,t}$, where i indicates the i-th segment $S^{i,\tau}_{v,t}$ it associates to, v and t corresponds to the vehicle and time the value being collected, and τ denotes a set of the time indices (e.g. $\tau = \{t_1, t_2, ..., t_n\}$) of the corresponding leakage segment.All pressure values of the leak segments $S^{i,\tau}_{V,T}$ of vehicle V over the period T are denoted as $X_{V,T}$. In this study, T is selected to be one day period. The parameters θ^i of the physics-based model f_{θ^i} are fitted over each segment $S^{i,\tau}_{v,t}$, minimizing squared errors between real pressure values and model prediction:

$$\underset{\theta^i}{\operatorname{argmin}} \left\| \left(\sum_{t \in \tau} f_{\theta^i}(t) - x^i_{v,t} \right) \right\|^2 \tag{9}$$

Fitted model parameters of all segments $S^{i,\tau}_{V,T}$ over time interval T of bus V were denoted as $\Theta_{V,T}$. For the non-elastic leakage model (equation 4), $\{k, \frac{L}{V}\}$ are the model parameters; for the elastic leakage model, $\{k, a, b\}$ are the parameters for model equation 5, and $\{m, n\}$ for model equation 8.

3.3 Computing Statistical Features

A conventional data-driven approach for fault detection would take statistical features of the raw sensor readings as the input to train a model. In this study, we investigate the usefulness of the fitted parameter of the three physics-based models, denoted as $\Gamma(\Theta_{v,t})$, and we compare them against the statistical features computed on raw sensor readings $\Gamma(X_{v,t})$.

For fitted parameters $\Theta_{V,T}$ of the physics-models and the raw pressure values $X_{V,T}$ collected from one bus V over one day period T, a set of statistical features $\Gamma(\cdot)$ were computed, including the arithmetic mean μ, the standard deviation σ, the 3rd and 4th standardized moments (Skewness $\frac{\mu_3}{\sigma_3}$ and Kurtosis $\frac{\mu_4}{\sigma_4}$), percentiles (the 10-th, 25-th, 50-th, 75-th, 90-th were selected), the entropy, and the root mean squared (RMS) values $\frac{1}{|T|}\sum_{t \in T}(x_t)^2$ (where $|\cdot|$ denotes the cardinality).

ANOVA F-test was conducted, and the F-score was used for ranking different types of features. In addition, machine learning models were trained with the two types of the features, i.e., $\Gamma(\Theta_{v,t})$ and $\Gamma(X_{v,t})$, and the area under the ROC curve were used for comparing the performance in discriminating the faulty samples (prior to air leak repair event) from the healthy sample (after repair was performed and the fault was dealt with).

4 Results

The results section is organized as follows: i) illustration of fitted physics-based models on the WTAP air leak segments; ii) visual inspection of fitted parameters of the physics-based models using box plot, focusing on two air leak cases; iii) comparing histograms of fitted parameters between the healthy and the faulty populations; iv) the ranking of the features with ANOVA F-score, and comparison of the area under the ROC curve.

Figure. 3 shows three example air leak segments and the corresponding fit of the three selected model equations. Since the sensor has a relatively low resolution, the pressure values are quantized into the levels shown. The two elastic models (Eq. 5 and Eq. 8) skew in different directions, while the non-elastic model behaves, in all three example segments, similarly to a linear model. For the elastic leakage model (equation 5), the parameter k and a corresponds to the leakage speed of the air pressure, while b corresponds to the offset of the segments; for the elastic leakage model (equation 8), m and n corresponds to the change in curvature of the fitted model; the fitting of parameters k and $\frac{L}{V}$ of the non-elastic leakage model (equation 4), which has a stronger constrain in the offset term compared to the model equation 5, leads to the term $\frac{LP_0}{V}$ dominating over the exponential decreasing term; therefore the fitted model behaves similarly to a linear model.

Table. 1 shows a set of box plots summarizing the fitted parameters $\Theta_{v,t}$ (of the three selected model equations, in rows) for the two air leak cases (in columns). The vertical solid lines mark the time of the repair action performed to fix the air leak fault. It can be observed that there is a clear distinction in the parameters b of model Eq. 5, as well as m and n of model Eq. 4, between

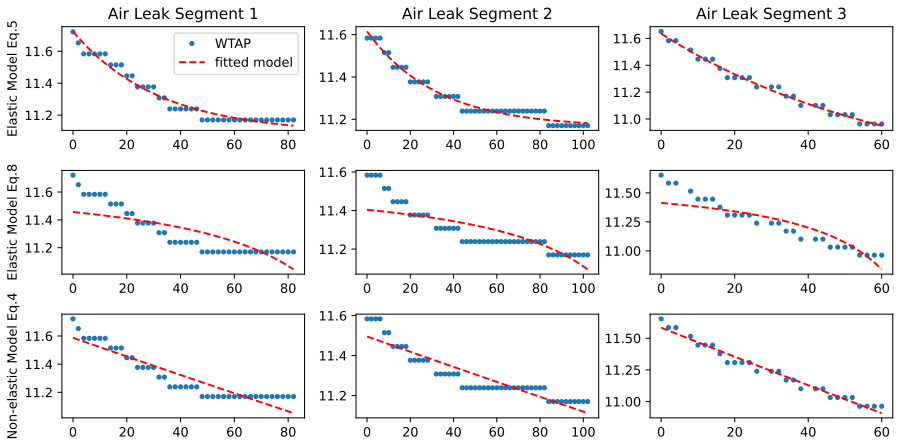

Fig. 3: Visual demonstration of the fitted parameters of three different physics-based models on three example air leak segments.

the faulty and healthy time periods in "Air Leak Case 2" (left column). It is also visible, in the right column, that there are obvious distinctions in the fitted parameter $\frac{L}{V}$ of model Eq. 8 and both parameters (m and n) of model Eq. 4 between the "before" and "after" the repair. Moreover, there are differences (albeit not obvious) in the model parameters (k and b of model Eq. 5) between healthy and faulty samples.

Table. 2 illustrates the difference in the distribution of selected statistical features $\Gamma(\Theta_{v,t})$ between healthy and faulty population. As is shown, there are obvious distinctions between the distribution of the mean, the RMS, and the three percentiles values of model parameter k of model Eq. 5, and $\frac{L}{V}$ of model Eq. 4.

Figure. 4 shows the ranking result of the ANOVA F-test (based on healthy and faulty samples of all six cases), comparing conventional statistical features $\Gamma(X_{v,t})$ on the raw data and the statistical features $\Gamma(\Theta_{v,t})$ of physics-inspired parameters, for all three model equations. The experiment was conducted with 6-fold cross-validation, in a leave-one-out setting, i.e. one failure case (and its corresponding three months of data) out of the six cases was left out of the training set non-repeatedly in each of the 6-fold cross-validation experiments; the error bars are generated correspondingly with the leave-one-out experiments. It is clear that overall, across all six air leak cases, most of the fitted parameters of the elastic model (Eq. 5) outrank the conventional features. Four fitted parameters of model Eq. 4 were placed in the top five features, while the fitted parameters of model Eq. 8 scored five features in the top 10 features. These results convincingly demonstrate the advantage of physics-inspired features over the raw sensor readings.

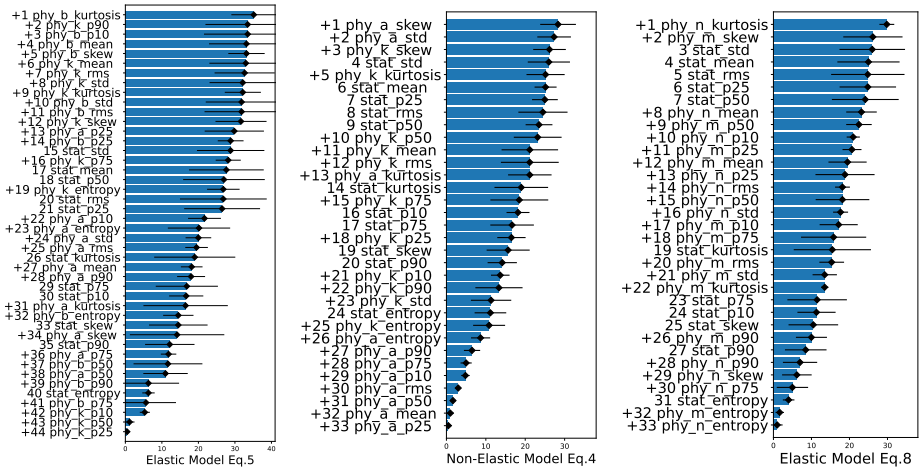

Fig. 4: Comparison of ANOVA F-score between features

Table 1: Illustration of evolution over time of the physics-based model parameters for two example air leak cases; the vertical solid lines mark the time of the air leak repair.

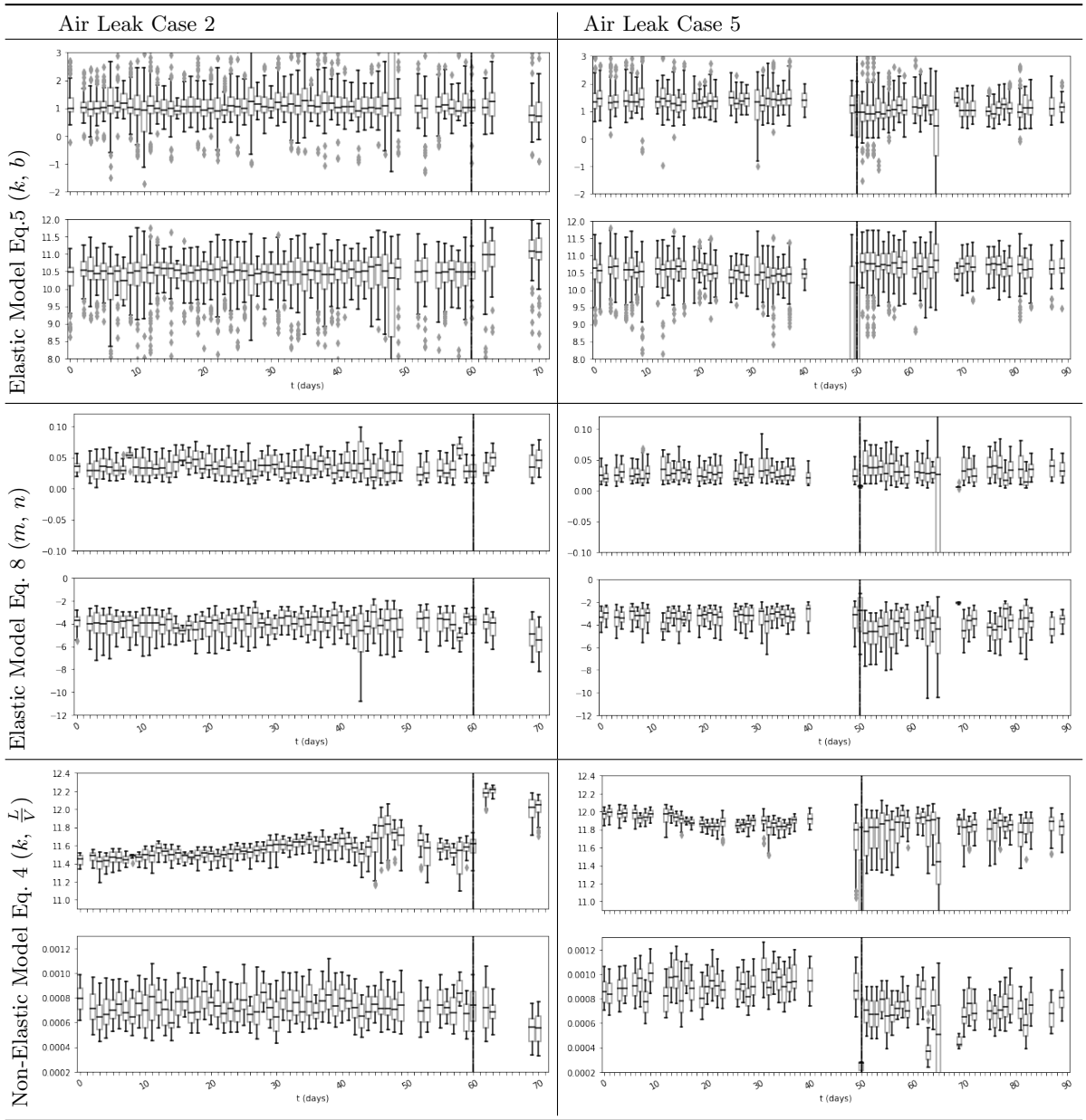

Table 2: PDF comparison of fitted parameters between "before" (red) and "after" (blue) air leak faults being treated in workshop (from case 5)

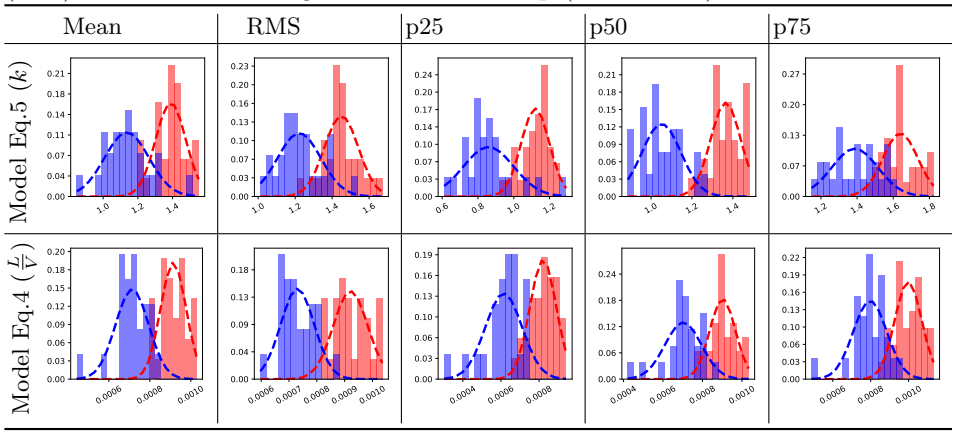

	$\Gamma(\Theta)$			$\Gamma(X)$
	Model Eq.5	Model Eq.4	Model Eq.8	WTAP
kNN	65.80±10.37	63.00±3.78	58.05±5.71	46.94±10.91
MLP	58.77±10.95	68.78±8.89	60.05±7.23	40.07±15.10

Table 3: Performance (AUC) comparison between using different features for discriminating faulty samples from fault-free samples, on all failures cases with 6-fold cross-validation.

The preliminary result, presented in Table. 3, of training and testing conventional machine learning models (k-Nearest-Neighbour (kNN) and multi-layer perception (MLP) classifier), with 6-fold cross-validation, shows that using the conventional features $\Gamma(X_{v,t})$ is not better than random guesses. The experiment was conducted in the same way as the result presented in Figure. 4. On the other hand, using the statistical features $\Gamma(\Theta_{v,t})$ on fitted parameters of the three physical models scored 65.80 ± 10.37 (model Eq. 5 with kNN), 68.78 ± 8.89 (model Eq. 4 with MLP), and 60.05 ± 7.23 (model Eq. 8 with MLP).

5 Conclusion and Future Work

In this study, we are exploring the use of physics-based air leakage models in generating useful features for detecting air leaks in city buses. We have compared the proposed physics-model-based features against the conventional ones and

showed a clear advantage of the proposed features. With the visual inspection of all box plots, we conclude that, in three out of the six air leak cases, there is a visible difference in the distribution of fitted parameters $\Theta_{v,t}$ between samples before and after the repair treated to the air leak faults. Although the box plot and histogram showed that there is a visual difference in the distribution of the features between the two classes (in half of the cases), the AUC indicated further efforts can be made to improve the performance, e.g. finding a proper learning setting for detecting the air leaks; further development on improving the fitting of physics-based air leak models by imposing relevant constraints for model fitting; exploring the vehicle service records for more air leak cases.

In this paper, only the detection of air leak faults was addressed and pressure values only during the idle state were used to estimate physical parameters. However, the air system is rather complicated, and the air pressure in the wet tank is affected by the usage of the end-use components. Therefore, a wider scope of this work is to consider the impact of all end-use components in the air system: design a comprehensive model that takes into account all possible operational states, i.e., activation associated with all end-use components, with respect to their physical process; utilizing fitted parameters of the physical models not only for detecting faults but also for fault isolation and identification, based on exploring the interpretability of the models; incorporating the fitted parameters into a data-driven fault detection and prognostic framework, utilizing deep learning methods for higher prediction performance.

6 Acknowledgments

This work was partially supported by Vinnova, Knowledge Foundation and by CHIST-ERA grant CHIST-ERA-19-XAI-012 funded by Swedish Research Council.

References

1. Davy, J.: Calculations for Leak Rates of Hermetic Packages. IEEE Transactions on Parts, Hybrids, and Packaging **11**(3), 177–189 (Sep 1975). https://doi.org/10.1109/TPHP.1975.1135069, conference Name: IEEE Transactions on Parts, Hybrids, and Packaging
2. Desai, A., Guo, Y., Sheng, S., Sheng, S., Phillips, C., Williams, L.: Prognosis of Wind Turbine Gearbox Bearing Failures using SCADA and Modeled Data. Annual Conference of the PHM Society **12**(1), 10–10 (Nov 2020). https://doi.org/10.36001/phmconf.2020.v12i1.1292, https://papers.phmsociety.org/index.php/phmconf/article/view/1292, number: 1
3. El Mir, H., Perinpanayagam, S.: Certification Approach for Physics Informed Machine Learning and its Application in Landing Gear Life Assessment. In: 2021 IEEE/AIAA 40th Digital Avionics Systems Conference (DASC). pp. 1–6 (Oct 2021). https://doi.org/10.1109/DASC52595.2021.9594374, iSSN: 2155-7209
4. Fan, Y., Nowaczyk, S., Rögnvaldsson, T.S.: Incorporating expert knowledge into a self-organized approach for predicting compressor faults in a city bus fleet. pp. 58–67 (2015)

5. Gálvez, A., Seneviratne, D., Galar, D.: Hybrid model development for hvac system in transportation. Technologies **9**(1), 18 (2021)
6. Lees, F.: Lees' Loss Prevention in the Process Industries: Hazard Identification, Assessment and Control. Elsevier Science & Technology, Oxford, UNITED STATES (2012), http://ebookcentral.proquest.com/lib/halmstad/detail.action?docID=1031883
7. von Rueden, L., Mayer, S., Beckh, K., Georgiev, B., Giesselbach, S., Heese, R., Kirsch, B., Walczak, M., Pfrommer, J., Pick, A., Ramamurthy, R., Garcke, J., Bauckhage, C., Schuecker, J.: Informed Machine Learning - A Taxonomy and Survey of Integrating Prior Knowledge into Learning Systems. IEEE Transactions on Knowledge and Data Engineering pp. 1–1 (2021). https://doi.org/10.1109/TKDE.2021.3079836, conference Name: IEEE Transactions on Knowledge and Data Engineering
8. Sepe, M., Graziano, A., Badora, M., Stazio, A.D., Bellani, L., Compare, M., Zio, E.: A physics-informed machine learning framework for predictive maintenance applied to turbomachinery assets. Journal of the Global Power and Propulsion Society **2021**(May), 1–15 (May 2021). https://doi.org/10.33737/jgpps/134845, https://journal.gpps.global/A-physics-informed-machine-learning-framework-for-predictive-maintenance-applied,134845,0,2.html, publisher: Global Power and Propulsion Society
9. Swischuk, R., Mainini, L., Peherstorfer, B., Willcox, K.: Projection-based model reduction: Formulations for physics-based machine learning. Computers & Fluids **179**, 704–717 (Jan 2019). https://doi.org/10.1016/j.compfluid.2018.07.021, https://www.sciencedirect.com/science/article/pii/S0045793018304250
10. Willard, J., Jia, X., Xu, S., Steinbach, M., Kumar, V.: Integrating scientific knowledge with machine learning for engineering and environmental systems. ACM Computing Surveys (CSUR) (2021)
11. Yucesan, Y.A., Viana, F.: A hybrid model for main bearing fatigue prognosis based on physics and machine learning. In: AIAA Scitech 2020 Forum. AIAA SciTech Forum, American Institute of Aeronautics and Astronautics (Jan 2020). https://doi.org/10.2514/6.2020-1412, https://arc.aiaa.org/doi/10.2514/6.2020-1412